

**Angular correlations and rotational motion in computer-simulated liquid nitrogen**

B. Quentrec and C. Brot

*Laboratoire de Physique de la Matière Condensée,\* Université de Nice, Parc Valrose, 06100-Nice, France*  
(Received 20 May 1974)

Further results of a "molecular dynamics" simulation of liquid nitrogen are described. These results have been obtained under triple-point conditions. A molecular-pair distribution function which depends on the radial distance, plus three angular variables, has been computed. Partial averages of this function are depicted. These functions show an angular structure up to about 9 Å, but are not sharply peaked. It seems that the orientation of a molecule is more influenced by the positions of its neighbors than by their orientations. The dynamics of the orientational motion has also been further studied. The coupling between the environment and the orientational behavior of a given molecule has been examined through both cross-correlation functions and selectively sampled correlation functions. These results are the following: (i) An initial high rotational temperature of the molecule facilitates its reorientation. (ii) An initial fluctuation of the local density affects the reorientational behavior of the molecule only if this fluctuation persists for a sufficiently long time. (iii) By contrast, there is little coupling between the behavior of a molecule and the rotational temperature of its interacting partners. (iv) Individual samples of the motion indicate that a molecule shares its time about equally between periods of orientational trapping, with erratic librational motion, and periods of continuous nonuniform rotation.

I. INTRODUCTION

In a recent paper<sup>1</sup> some static and dynamic properties of a computer-simulated homonuclear liquid were described. The aim of this paper is to present several new results on the same system.

The two-atom potential used is the same as the one that we proposed a few years ago<sup>2</sup> and that was employed in Ref. 1, the centers of action of the Lennard-Jones forces coinciding with the centers of mass of the atoms.

The number of molecules and also the integration procedure remain the same. More elaborate statistical averages have been devised, in order to obtain more detailed information about both the static angular correlations of the molecules and their orientational self-motion. We briefly recall the parameters we use: An atom-atom potential

$$U_{ij} = \sum_{n=1}^4 v(r_n), \tag{1}$$

where  $r_n$  is the distance between two unbounded atoms in molecules  $i$  and  $j$  and where  $v(r_n)$  is the Lennard-Jones potential

$$v(r_n) = 4\epsilon[(\sigma/r)^{12} - (\sigma/r)^6] \tag{2}$$

with  $\epsilon = 0.6067 \times 10^{-14}$  ergs and  $\sigma = 3.341$  Å. The interatomic distance in a molecule is  $2d$  with  $d = 0.1646\sigma$ . These values are adequate to simulate nitrogen.<sup>1</sup> Moreover, we have computed the equipotential curves for the interaction between a molecule and a supposedly independent atom of another molecule, i.e.,  $v(\vec{r} - \vec{r}_A) + v(\vec{r} - \vec{r}_{A'})$  where  $\vec{r}_A$  and  $\vec{r}_{A'}$  are the positions of the atoms of the molecule

and  $\vec{r}$  the position of the supposedly independent atom. These equipotentials are reproduced in Fig. 1. We can (somewhat arbitrarily) define the shape of the molecule as the inner envelope of the family of circles with radius  $\frac{1}{2}\sigma$  centered on the equipotential zero. This envelope is indicated in Fig. 1. Its shape is very similar to that of the outer electron-density curves of nitrogen.<sup>3</sup> We note also that the lower equipotentials, which are the

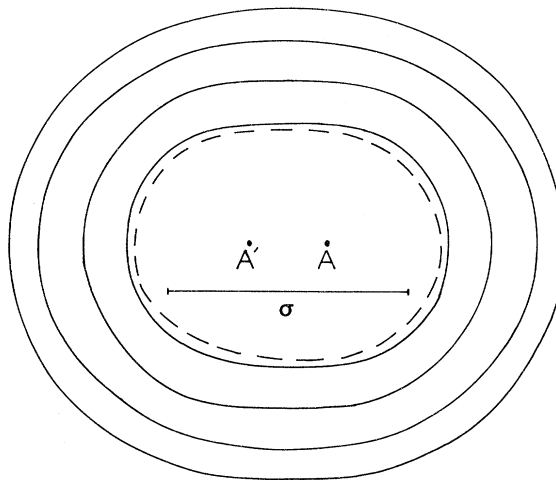


FIG. 1. Equipotential curves for the interaction between a molecule and a supposedly independent atom of another molecule, i.e.,  $v(\vec{r} - \vec{r}_A) + v(\vec{r} - \vec{r}_{A'})$ , where  $\vec{r}_A$  and  $\vec{r}_{A'}$  are the position of the atoms  $A$  and  $A'$  of the molecule and  $\vec{r}$  is the position of the supposedly independent atom. The unit length  $\sigma$  is given on the figure. Solid line from outside to inside, equipotentials: 0, 20, 400, 14 000. Dashed line: shape of the molecule from outer electron density curves, Ref. 3.

only ones represented in Fig. 1, do not have a dumbbell shape (they would be dumbbell shaped only for high potentials which are not reached during the interactions at the pressure and temperature we consider here).

The computation was done using the following conditions: Number of molecules in the cubic box —500, with periodic boundary conditions. We denote by  $\tilde{u}_j$  a *unit* vector along the axis of molecule  $j$ . The temperature  $T^*$  will be given in units of  $\epsilon/k_b$ , where  $k_b$  is the Boltzmann constant, the pressure  $P^*$  in the units of  $\epsilon\sigma^{-3}$ , the distances in units of  $\sigma$ , and the number densities  $\rho^*$  in units of  $\sigma^{-3}$ . For nitrogen, with the above potential, we have, at triple point,

$$T^* = 1.437, \quad \rho^* = 0.696, \quad P^* = 7.7 \times 10^{-4};$$

and at the critical point,

$$T^* = 2.86, \quad \rho^* = 0.246, \quad P^* = 0.22.$$

## II. MOLECULAR PAIR-DISTRIBUTION FUNCTION

In Ref. 1, the *atomic* pair-distribution function for a homonuclear diatomic liquid is defined and its behavior is described. This function is convenient for interpreting scattering experiments since the scattering centers are the nuclei for neutrons or the essentially spherical high electronic density region of each atom for x rays.

It is remarkable that this atom-atom pair-distribution function is in excellent agreement with the one deduced from x-ray diffraction<sup>4</sup> (see, for example, the two atomic structure factors compared in Fig. 7 of Ref. 1).

Since the publication of Ref. 1, two more pieces of information have become available. The first one is a neutron-diffraction study by Dore, Walford, and Page.<sup>5</sup> These authors report an atom-atom structure factor which is also in good agreement with that of Ref. 4, hence also with our computed curve. Perhaps more enlightening for the understanding of the phenomena involved is a theoretical study by Lowden and Chandler<sup>6</sup> who consider "fused hard sphere molecules." They treat a liquid composed of such molecules by the so-called reference-interaction-site model method, which consists essentially in writing an Ornstein-Zernike-like equation for the atoms (this equation involves an intramolecular pair-correlation function) and in assuming that the direct correlation function vanishes outside the hard-core atomic diameter. They finally compare their results for the structure factor with those of Ref. 1 by introducing an "effective diameter" which corrects for the non-hard character of the repulsive part of our site-site Lennard-Jones potential; this comparison

(see their Fig. 11) is rewarding. This stresses the fact that at high density the repulsive part of the potential is the main factor governing the structure, in atom-atom Lennard-Jones fluids as well as in real molecular fluids. This remark is parallel to a fact now well known in monatomic fluids; it renders suspect the use of electric forces only (e.g., quadrupoles) for depicting the anisotropic interactions in molecular liquids or crystals.

Although diffraction experiments yield only the atom-atom structure factor or distribution function for homonuclear molecules, a complete description of the intermolecular arrangement requires the knowledge of a function depending on several variables, including the relative orientations of the molecules. This leads us to define and study *molecular* pair-distribution functions.

In order to do this, the familiar pair-correlation function of monatomic liquids needs to be generalized to the case of molecular liquids in which the angular degrees of freedom must be taken into account. In the most general case (molecules of symmetry 1) one should define the pair-correlation function  $g_M$  through

$$\rho(r, \theta, \varphi, \theta_j, \varphi_j, \psi_j) = \frac{\rho}{8\pi^2} g_M(r, \theta, \varphi, \theta_j, \varphi_j, \psi_j). \quad (3)$$

Here  $r$ ,  $\theta$ , and  $\varphi$  are the spherical polar coordinates of the vector  $\vec{r}$  joining the center of mass of the central molecule to that of molecule  $j$ , in a reference frame bound to the central molecule.  $\theta_j$ ,  $\varphi_j$ , and  $\psi_j$  are the angles defining the orientation of the molecule  $j$  in a reference frame equipollent to the first.  $\rho(r, \theta, \varphi, \theta_j, \varphi_j, \psi_j) dr \sin\theta d\theta d\varphi \times \sin\theta_j d\theta_j d\varphi_j d\psi_j$  is the probability of finding a molecule in  $d\vec{r}$  at  $\vec{r}$  with orientation in  $\sin\theta_j d\theta_j \times d\varphi_j d\psi_j$  about  $\theta_j, \varphi_j, \psi_j$ .

It is obviously convenient to choose the first reference frame along the axis of inertia of the central molecule.  $\rho$  is the mean number density, so that at large  $r$ , where angular correlations are lost,  $g_M$  tends towards unity.

If we are not interested in, say, the dependence on the precession angle  $\psi$  we define

$$\rho'_M(r, \theta, \varphi, \theta_j, \varphi_j) dr \sin\theta d\theta d\varphi \sin\theta_j d\theta_j d\varphi_j$$

as the probability of finding a molecule in  $d\vec{r}$  at  $\vec{r}$  with its principal axis of inertia oriented into  $\sin\theta_j d\theta_j d\varphi_j$  about  $\theta_j, \varphi_j$ .

This is obviously the case for linear molecules, for which  $\psi$  is meaningless. Comparing with Eq. (3) we have<sup>7</sup>

$$\rho'_M(r, \theta, \varphi, \theta_j, \varphi_j) = \frac{\rho}{4\pi} g_M(r, \theta, \varphi, \theta_j, \varphi_j). \quad (4)$$

In  $\rho'_M$  we have dropped the argument  $\varphi$  since, because of the symmetry of the potential, the dependence of the above quantities on  $\varphi$  disappears. Also we can no longer choose the origin of  $\varphi$  by reference to the orientation of the central molecule. Instead we have chosen an axis in the plane defined by  $\vec{OZ}$  and  $\vec{r}$  (see Fig. 2).

We have

$$g_M(r, \theta, \theta_j, \varphi_j) = g_M(r, \theta, \pi - \theta_j, \varphi_j + \pi) \quad (5)$$

from the inversion center of molecule  $j$ ;

$$g_M(r, \theta, \theta_j, \varphi_j) = g_M(r, \pi - \theta, \pi - \theta_j, -\varphi_j) \quad (6)$$

from the inversion center of the central molecule; and

$$g_M(r, \theta, \theta_j, \varphi_j) = g_M(r, \theta, \theta_j, -\varphi_j), \quad (7)$$

where we have made use of the symmetry, with respect to the plane  $\vec{Oz} \vec{r}$ , of the potential exerted by the central molecule on molecule  $j$ . From Eqs. (5)–(7), it is seen that it is sufficient to know

$$g_M(r, \theta, \theta_j, \varphi_j) \quad \text{for } 0 \leq \theta \leq \frac{1}{2}\pi, 0 \leq \theta_j \leq \frac{1}{2}\pi, 0 \leq \varphi_j \leq \pi. \quad (8)$$

$g_M(r, \theta, \theta_j, \varphi_j)$  has been extracted from the computer simulation for conditions corresponding closely to the triple point. This has been done for ten equally spaced values of  $r$  between 0.1 and 1.5 $\sigma$  and for ten equally spaced values from 1.5 to 2.5 $\sigma$ .

The increment of the angles, computed in the ranges defined by the inequalities (8), was  $\frac{1}{12}\pi$ . The full table of the data, comprising 8640 numbers, cannot be given here.<sup>8</sup> We describe only, in the form of several figures, the most characteristic results.

Figure 3 shows, for three different sets of the

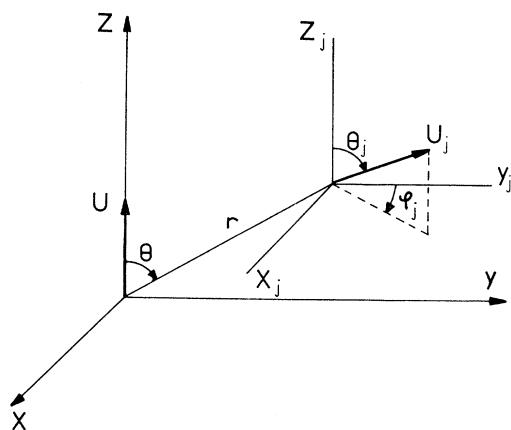


FIG. 2. Frame of reference used to define  $g_M(r, \theta, \theta_j, \varphi_j)$ . The axes  $x_j, y_j, z_j$  are respectively parallel to the axes  $x, y, z$ .  $\vec{r}$  is in the plane defined by the axes  $y$  and  $z$ . For convenience of calculation  $\varphi_j$  is defined in an unusual way.

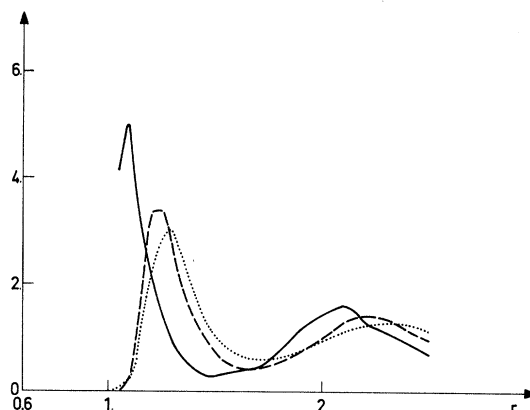


FIG. 3. Molecular pair-distribution function  $g_M(r, \theta, \theta_j, \varphi_j)$  for liquid nitrogen near the triple point for three different values of the angles  $(\theta, \theta_j, \varphi_j)$ . Solid line  $g_M(r, 90^\circ, 90^\circ, 90^\circ)$ , dashed line  $g_M(r, 0^\circ, 90^\circ, 0^\circ)$ , dotted line  $g_M(r, 37^\circ 5', 67^\circ 5', 37^\circ 5')$ .

angles  $\theta, \theta_j, \varphi_j$ , the function  $g_M(r, \theta, \theta_j, \varphi_j)$  vs  $r$ . For all three cases the function has an important first peak which corresponds to the first shell of neighbors. The abscissa of the first peak varies with the direction  $\theta$  and the relative orientation  $\theta_j, \varphi_j$ , as expected from steric effects: for example, the position of the first peak of  $g_M(r, 0, \frac{1}{2}\pi, \varphi_j)$  differs by half the interatomic distance  $d$  from that of  $g_M(r, \frac{1}{2}\pi, \frac{1}{2}\pi, \frac{1}{2}\pi)$ . One can understand in the same way that the abscissa of the first peak in  $g_M(r, \frac{1}{2}\pi, \frac{1}{2}\pi, \varphi_j)$  varies approximately as  $\cos \varphi_j$ . However, it is not possible to explain in such a simple way the differences between the peak heights of the different curves. For larger  $r$  the molecular pair-distribution function shows smoother oscillations, which still persist at  $r = 2.5$ .

We have computed further angular averages:

$$g_1(r, \theta) = \frac{1}{4\pi} \int_0^{2\pi} d\varphi_j \int_0^\pi g_M(r, \theta, \theta_j, \varphi_j) \sin \theta_j d\theta_j, \quad (9)$$

$$g_2(r, \theta_j) = \frac{1}{4\pi} \int_0^{2\pi} d\varphi_j \int_0^\pi g_M(r, \theta, \theta_j, \varphi_j) \sin \theta d\theta. \quad (10)$$

These functions are represented in perspective in Figs. 4 and 5. Since the number of computed points was not sufficient to draw an apparently continuous curve, an interpolation process has been used which splits the discontinuities into many small steps; however, when the variation of the function is rapid, these steps are still visible; they have, of course, no physical reality.

The angular structure of  $g_1(r, \theta)$  is clearly observable in Fig. 4. The crest at the back of the figure corresponds to the first shell of neighbors; it has two flat maxima at  $\theta = 37.5^\circ$  and  $90^\circ$ , separat-

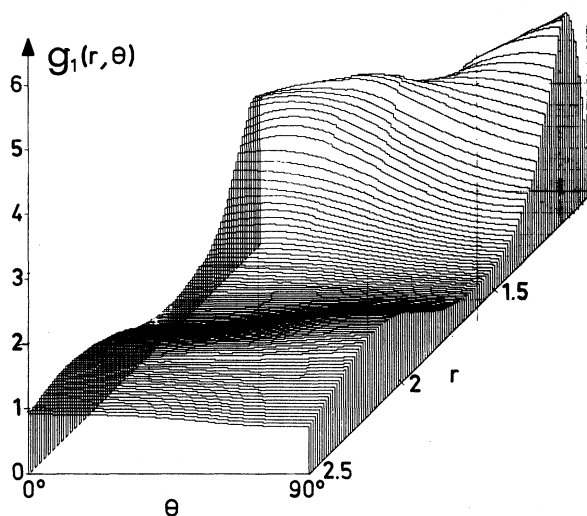


FIG. 4.  $g_1(r, \theta)$  for liquid nitrogen near the triple point.  $\theta$  increases from left to right and  $r$  towards the front of the figure.

ed by flat saddle points at  $\theta=0^\circ$  and  $45^\circ$ . It is remarkable that the maxima have angular positions  $\theta$  close to those of the  $\delta$  distributions ( $35^\circ 10'$  and  $90^\circ$ ) which correspond to the equilibrium configuration<sup>9</sup> of crystalline nitrogen in phase  $\alpha$ ; also the relative heights of these peaks are in the same order as for the  $\delta$  distributions. As expected, this correspondence is even more pronounced for solid  $\alpha$ -nitrogen itself at finite temperature (see following paper). This angular structure is, of course, a collective effect (as in the crystalline phase), since the two-body potential varies monotonically between  $0^\circ$  and  $90^\circ$  (see Fig. 1). For larger  $r$ , the second shell of neighbors, between  $2.1$  and  $2.2\sigma$ , appears, but its angular structure is rather less pronounced. This structure still persists at  $r = 2.5\sigma$ . Figure 5 represents  $g_2(r, \theta_j)$ . It is less

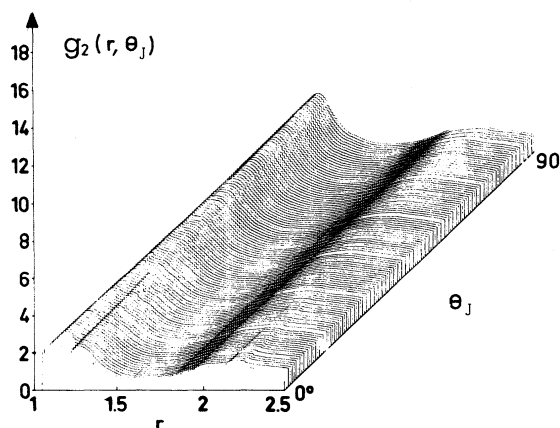


FIG. 5.  $g_2(r, \theta_j)$  for liquid nitrogen near the triple point.  $r$  increases from left to right and  $\theta$  towards the back of the figure.

structured than  $g_1$ . The first shell of neighbors exhibits little dependence on  $\theta_j$  (near  $\theta_j=0$  it is split into two close maxima; we have no explanation to offer for this phenomenon).

In summary, the angular correlations in simulated liquid nitrogen near the triple point exist, recall the structure of the  $\alpha$  solid, but are not sharply peaked, probably because of the small elongation of the molecules. The fact that  $g_1$  is more structured than  $g_2$  indicates that the neighboring molecules impose preferred orientations on the reference molecule more through the configuration of their centers of mass than through their own orientations. In other words, the reference molecule "sees" essentially a monatomic fcc structure, but all other remnants of the particular space group of the  $\alpha$  phase ( $Pa_3$ , which is face-centered for the centers of mass) have almost disappeared. This can perhaps be put in parallel with the fact that the angular freedom is high in the  $\alpha$  phase, and also with the fact that this phase does not remain the most stable at higher temperatures, since a "plastic"  $\beta$  phase exists.

Averaging now the angular structure, we recall that the previously<sup>1</sup> computed pair-correlation function<sup>7</sup>:

$$g_M(r) = \frac{1}{2} \int_0^\pi g_1(r, \theta) \sin \theta d\theta \quad (11)$$

becomes the usual pair-correlation function for spherical molecules. It shows a behavior similar to that of a monatomic liquid<sup>1</sup> and reaches practically its asymptotic value 1, at  $r=3.2$ . The first shell of neighbors [up to the first minimum in  $g_M(r)$ ] includes 11.5 molecules.<sup>1</sup>

The detailed angular arrangement depicted in this section cannot be checked against a single diffraction experiment. However, the predominantly  $Pa_3$ -like angular arrangement we find is not in contradiction with diffraction results since, as the authors of Ref. 5 put in their conclusions, "Neither the uncorrelated nor the perpendicular correlation models are in satisfactory agreement with the data, and although the parallel orientation model gives satisfactory results it is not expected to be a very plausible model of the liquid structure."

### III. ORIENTATIONAL SELF-MOTION AND ITS DEPENDENCE ON THE FLUCTUATIONS OF THE MOLECULAR ENVIRONMENT

In Ref. 1 several time-correlation functions (CF) were given—in particular, the vector CF,  $\langle \tilde{u}_i(0) \cdot \tilde{u}_i(t) \rangle$ , and the tensor CF,  $\frac{1}{2} \langle 3[\tilde{u}_i(0) \cdot \tilde{u}_i(t)]^2 - 1 \rangle$ . Here we will call these functions  ${}_1F_u(t)$  and  ${}_2F_u(t)$ , respectively, in order to have a notation easily generalized for correlation functions of spherical

harmonics of higher orders (these are useful for the interpretation of neutron inelastic scattering experiments, for example).<sup>10</sup>

For a really homonuclear diatomic molecule there exists no experimental means of obtaining  ${}_1F_u(t)$ , so that our results cannot be checked against experiment; however the knowledge of the behavior of the simplest CF describing the orientational behavior is obviously enlightening; moreover, this function would be the one pertinent for interpreting ir absorption in unsymmetrical molecules of similar shape such as CO.

${}_1F_u(t)$  and  ${}_2F_u(t)$  have been shown<sup>1</sup> to depart only slightly from free rotation behavior up to  $0.2 \times 10^{-12}$  sec, then decrease more slowly; this decay takes an exponential form from  $t \approx 0.5 \times 10^{-12}$  sec onwards.  ${}_1F_u(t)$  is reproduced in Fig. 8 (solid line); the absolute error in it is 0.01, except in the tail where it reaches 0.02. The behavior of  ${}_1F_u(t)$  has been quantitatively compared to that predicted by different models.<sup>1,11</sup> We will now correlate this behavior with the fluctuations in the local environment of the test molecule. We have made this study using near triple-point conditions ( $T^* = 1.47$ ,  $\rho^* = 0.696$ ).

#### A. Description of the environmental fluctuations

We will call "interacting partners" any two molecules whose shortest atom-atom distance is smaller than some value  $l_0$ . This definition takes into account, in a way, the shape of the molecule; it seems preferable, for the present purpose, to a definition using the distance between the centers of mass. At a given instant of time  $t$ , molecule  $i$  has  $N_i(t)$  "partners" defined in this way. We have chosen  $l_0 = 1.2\sigma$ ; this value corresponds<sup>1</sup> to the middle of the first peak in the atomic pair-distribution  $g_A(r)$ ; also this value is close to the abscissa of the minimum in the potential of Eq. (2), so that it can be said that  $N_i(t)$  is the number of molecules interacting strongly with molecule  $i$ .

Dropping now the subscript  $i$ , we give in Table I the statistical distribution of  $N(t)$ : its mean value is 8.84 and its variance  $\sigma_N^2$  is 1.7. It is worthwhile

noting the importance of the wings of the distribution: 11% of the molecules have 7 "partners" or less; almost 10% have 11 "partners" or more.

We have computed the autocorrelation function of the fluctuations of  $N(t)$

$$F_N(t) = \frac{\langle [N(0) - \langle N \rangle][N(t) - \langle N \rangle] \rangle}{\sigma_N^2}. \quad (12)$$

This CF is represented in Fig. 6; the error on it is 0.01 (0.02 in the tail). This tail is remarkably long; at  $t = 3 \times 10^{-12}$  sec,  $F_N(t)$  still has the value 0.05. We have sampled several molecules and observed individually their behavior: for some of them  $N(t)$  remained larger than 10 during times as long as  $3 \times 10^{-12}$  sec. Since it is unlikely that a given molecule remains in a high-density environment while exchanging its partners, one is led to conclude that some persistent clustering of the molecules can exist. Such a clustering cannot be an artifact resulting from an incomplete "melting" of the initial solid. In order to ensure this, we first increased both the size and the temperature of the box during some 150 steps before returning to the desired conditions. The total working run lasted 1800 steps of  $10^{-14}$  sec.

At each instant of time we also computed the mean square of the angular momentum  $J$  of the  $N$  partners of molecule  $i$ . This was then divided by  $2I$ , where  $I$  is the moment of inertia of the molecule; the result  $R(t)$  can be termed the instantaneous rotational temperature of the partners. Its time-averaged value was as expected equal to  $T^* = 1.47$ . Its variance is  $\sigma_R = 0.50$ ; its distribution is given in Table I. The time-correlation function of  $R(t)$  is shown in Fig. 6. The relaxation of this function is faster than that of  $N(t)$ .

#### B. Further results on one-molecule rotational dynamics

We have computed the normalized ACF for the instantaneous rotational temperature, i.e.,

$$F_{J^2}(t) = \langle J^2(0)J^2(t) \rangle / \langle J^4(0) \rangle. \quad (13)$$

It is easily shown, using the Boltzmann distribu-

TABLE I. Statistical distribution of  $N(t)$ :  $P_N$  is the probability to find at a given time  $t$  a number  $N$  of "interacting partners" for a given molecule. Statistical distribution of  $R(t)$ :  $P_R$  is the probability for the "interacting partners" to have an instantaneous rotational temperature  $R$  at a given time  $t$ .

Statistical Distribution of $N(t)$										
$N$	4	5	6	7	8	9	10	11	12	13
$P_N$	0.001	0.007	0.030	0.107	0.236	0.309	0.218	0.079	0.012	0.001
Statistical Distribution of $R(t)$										
$R$	0.7	0.9	1.1	1.3	1.5	1.7	1.9	2.1	2.3	2.5
$P_R$	0.051	0.106	0.151	0.169	0.153	0.125	0.090	0.060	0.036	0.021

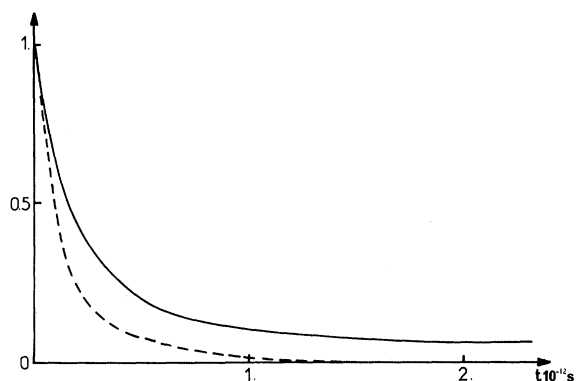


FIG. 6. Self-correlation function of the environment fluctuations. Solid line  $F_N(t)$ ; dashed line  $F_R(t)$ .

tion for the angular momentum, that the asymptotic value of this function is  $\frac{1}{2}$ . This function is represented in Fig. 7; for comparison,  $F_J(t)$ , already published in Ref. 1, is also reproduced. It is seen that the decay of  $F_{J^2}(t)$  is slightly slower than that of  $F_J(t)$ . Figure 8 shows the cross-correlation function (CCF)

$${}_1F_{uJ^2}(t) = \frac{\langle J^2(0)\tilde{u}(0) \cdot \tilde{u}(t) \rangle}{\langle J^2 \rangle} \quad (14)$$

together with the ACF  ${}_1F_u$ . It is seen that the CCF decays faster, indicating that a molecule which has a high initial rotational temperature has more chance of rapidly randomizing its orientation. The error on the functions  $F_J$ ,  $F_{J^2}$ ,  ${}_1F_{uJ^2}$  is also 0.01 (0.02 in the tails).

### C. Cross correlations with the environment

Here the word environment is used to mean the set of partners of a given molecule, as defined in Sec. IIIA. Let us first consider the distribution

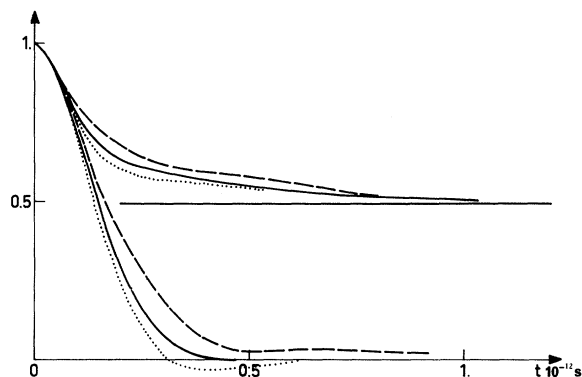


FIG. 7. Self-correlation function and density selectively sampled correlation function of the angular momentum  $\vec{J}$  and of its square  $J^2$ . Lower curve—solid line:  $F_J(t)$ ; dashed line:  $F_J^2(t)$  for  $N_I=7$ ; dotted line:  $F_J^2(t)$  for  $N_s=10$ . Upper curves—similar to lower curves for  $J^2$ .

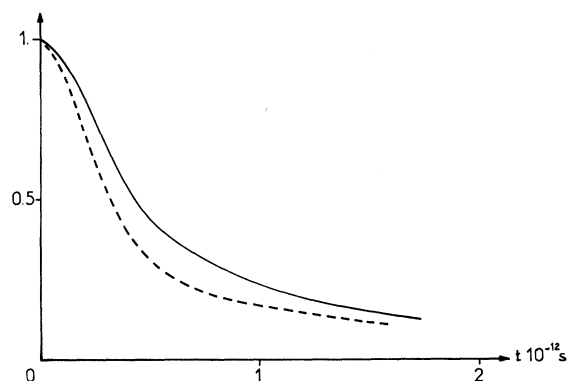


FIG. 8. Influence of the initial rotational temperature on the disorientation of the molecule. Solid line:  ${}_1F_u(t)$ ; dashed line:  ${}_1F_{uJ^2}(t)$ .

of the individual rotational temperatures  $J^2/2I$ . Its variance is easily shown to be  $k^2T^2$ . This gives  $2.16\epsilon^2$  at the temperature we have studied. Our “experimental” figure  $2.2\epsilon^2$  agrees well with the theoretical one. If the individual rotational temperatures of the molecules were random independent variables, then  $R(t)$  [the mean of  $\langle N(t) \rangle \approx 9$  such variables] would have a variance  $2.16/9 = 0.24$ . Its exact value, 0.25, does not differ much from this figure. Hence, the rotational temperatures of interacting molecules are *not* strongly coupled. We have verified this fact by computing the cross-correlation function:

$$F_{R,J^2} = \frac{\langle [R(0) - \langle R \rangle][J^2(t) - \langle J^2 \rangle] \rangle}{\sigma_R \sigma_{J^2}} \quad (15)$$

This CCF remains small at all times (see Fig. 9) and is almost at the limit of our statistical errors, whose absolute value is again 0.01.

In contrast, there exists a correlation between the time evolution of the rotational temperature of a molecule and that of the local density around

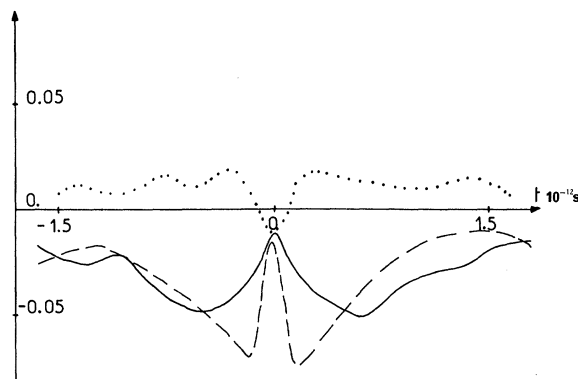


FIG. 9. Cross-correlation function of the environment fluctuations. Solid line:  $F_{N,R}(t)$ ; dashed line:  $F_{N,J^2}(t)$ ; dotted line:  $F_{R,J^2}(t)$ . The statistical error is  $\leq 0.01$ .

it: we have computed the CCF

$$F_{N, J^2} = \frac{\langle [N(0) - \langle N \rangle][J^2(t) - \langle J^2 \rangle] \rangle}{\sigma_N \sigma_{J^2}}, \quad (16)$$

which is represented in Fig. 9. This curve exhibits a sharp minimum at  $t = 0.15 \times 10^{-12}$  sec. This indicates that if the initial density is high, the molecule tends to first cool during this span of time, and thermalize again afterwards; the converse is also true. Surprisingly enough, no significant cross correlation was found between the initial density and the change in orientation at time  $t$ :  $F_{N, u} = \langle N(0)\vec{u}(0) \cdot \vec{u}(t) \rangle / \langle N \rangle$  has been found to be practically identical to  ${}_1F_u(t)$ . We will come back to this question in Sec. III D.

We have also computed the following cross correlation for the environment:

$$F_{N, R}(t) = \langle [N(0) - \langle N \rangle][R(t) - \langle R \rangle] \rangle / \sigma_N \sigma_R. \quad (17)$$

This function, which is also plotted in Fig. 9, exhibits the same kind of behavior as  $F_{N, J^2}$ . Its time variation is smoother, probably because the local density, here defined as seen from molecule  $i$ , is not the same at the same instant of time for its partners, so that the correlation is somewhat blurred.

#### D. Selectively sampled correlation functions

Let  $A_i(t)$  be some operator associated with molecule  $i$ . Let us define

$$F_A^S(t) = \frac{\int_0^\infty \sum_{i \in D} A_i(s) A_i(s+t) ds}{\int_0^\infty \sum_{i \in D} A_i^2(s) ds},$$

where  $s$  is the time.  $D$  is a set of molecules which both at  $s$  and at  $s+t$  satisfy some conditions. The set  $D$  depends on  $s$  and  $t$ , but at equilibrium, the number of molecules in  $D$  is stationary with respect to  $s$ . We will choose for the definition of  $D$ , the set of molecules which have *at least* some numbers  $N_s$  of "partners." We define  $F_A^I(t)$  analogously by choosing for  $D$  the set of molecules having *at most*  $N_I$  "partners." Of course, it can happen that a molecule is in  $D$  at time  $s_0$ , but not in it at  $s_1$ , and is in it again at  $s_2$  ( $s < s_0 < s_1 < s_2 < s+t$ ), but this situation will seldom appear for  $t$  smaller than the relaxation time of  $N(t)$  ( $\approx 0.5 \times 10^{-12}$  sec), so that it can be said that  $F_A^S(t)$  [ $F_A^I(t)$ ] is essentially a CF of  $A_i(t)$  sampled on molecules which have remained in an environment of high [low] density. Choosing  $N_s = 10$ , the fraction of molecules belonging to  $D$  is 0.31 at  $t=0$ , and is 0.14 at  $t = 0.3 \times 10^{-12}$  sec; it is 0.104 at  $t = 3 \times 10^{-12}$  sec and its asymptotic value is obviously  $(0.31)^2 = 0.0961$ .

Since, for computing the following "selectively sampled correlation functions," the statistics bear on only a fraction of the total number of molecules

(typically 100 instead of 500), our absolute error reaches 0.03.

$F_J^S(t)$  and  $F_J^I(t)$  have been computed and are compared with  $F_J(t)$  in Fig. 7; the negative part exhibited by  $F_J^S(t)$  indicates that there exists, for molecules at high density, a phenomenon of rebound against their neighbors. This fact indicates the existence of some librational character in the motion of molecules in dense environments; we have explored qualitatively the nature of this phenomenon and will discuss it in Sec. III E.

The density-selected orientational correlation functions  ${}_1F_u^S(t)$  and  ${}_1F_u^I(t)$  have also been computed and are reproduced in Fig. 10. It is clearly seen that the reorientations are fast if the local density remains low and slow if this density remains high. A rapid initial fluctuation in the density is not sufficient to change the reorientational behavior, as already mentioned in Sec. III C. We have also computed functions  ${}_1F_u^{S'}$  and  ${}_1F_u^{I'}$ , where the set  $D$  is now defined by reference to the local rotational temperature  $R(t)$  instead of the density. We found no significant difference between  ${}_1F_u^{S'}(t)$ ,  ${}_1F_u^{I'}(t)$ , and  ${}_1F_u^S(t)$ . The same negative result was found for  $F_J^S(t)$  and  $F_J^I(t)$ . This shows that the local rotational temperature has no influence on the rotational behavior of the reference molecule. This is in agreement with the small value always found for the CCF  $F_{R, J^2}$ .

Finally, we mention that another run of molecular dynamics performed at smaller density and higher temperature ( $\rho^* = 0.65$ ,  $T^* = 2.05$ ) has shown a much freer rotational behavior in which the selectively sampled CF's were found to be identical to the ordinary ones. Also one should remember that the nitrogen molecule does not have a very large anisotropy in its interaction potential. For

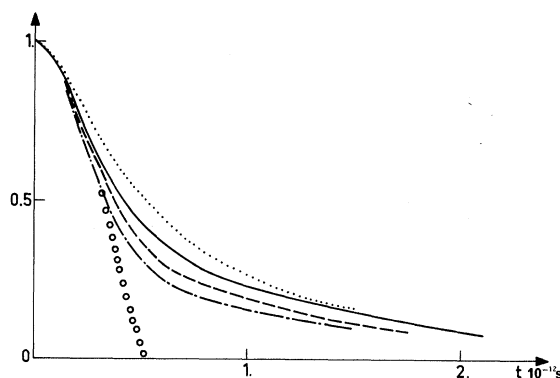


FIG. 10. Density selectively sampled correlation function for the orientation vector  $\vec{u}$ . Solid line:  ${}_1F_u(t)$ ; dotted line:  ${}_1F_u^S(t)$  for  $N_s=10$ ; dashed line:  ${}_1F_u^I(t)$  for  $N_I=8$ ; dot-dashed line:  ${}_1F_u^I(t)$  for  $N_I=7$ ; open circles: free rotation at the triple-point temperature.

more elongated or complicated molecules the results we have observed would probably not be valid.

#### E. Discussion

Considering first the various autocorrelation functions ( ${}_1F_u$ ,  $F_J$ ,  $F_{J^2}$ ,  $F_N$ ) whose behavior was reported above, an obvious statement is that their correlation times are of the same order of magnitude: these times fall between  $0.2 \times 10^{-12}$  and  $0.6 \times 10^{-12}$  sec.

We will now make a brief comparison between our results and several typical models proposed in the literature, but at this point a preliminary remark on this comparison seems in order: most models envisage some limiting cases, e.g., cases where some of the coupled dynamical variables randomize much faster than others. This is not the situation we observe in computer-simulated nitrogen, where all the variables concerning one molecule vary smoothly on comparable times scales. To illustrate this we present in Fig. 11 a sample of the time variation of two dynamical variables pertaining to the same molecule, during a time span of  $7.5 \times 10^{-12}$  sec. These variables are the cosine of the orientation angle with respect to a fixed axis and the squared angular momentum. Whereas it is apparent that the rate of change of the latter is faster than that of the former, it remains true that no strong inequality between their correlation times exists.

Although this situation evokes some sort of smooth molecular chaos, the influence of density fluctuations on orientational behavior, which has been inferred from both our cross-correlation

functions and our selectively-sampled correlation functions, produces some structure in the orientational motion. This structure is visible on the cosine  $\theta$  curve of Fig. 11: On the right-hand side of the figure, during a stage that lasts at least  $3 \times 10^{-12}$  sec, the molecule remains more or less trapped along the direction  $\theta=0$ , performing an erratic librational motion with an average amplitude of some  $15^\circ$ ; in between such stages the molecule has a regime of large-angle nonuniform rotation. We have checked that this situation is real by examining the behavior of some twenty molecules during  $10^{-11}$  sec.<sup>12</sup> As far as they can be exactly defined, the stages of trapping and those of large-angle rotation range from  $0.2$  to  $0.8 \times 10^{-12}$  sec. On average they have about equal weight, but the molecules with a long-lasting high number of partners have longer periods of trapping.

We now proceed to the examination of the degree of validity of the most well-known models in the literature when applied to computer-simulated nitrogen. We observe the following.

(1) Free, i.e., "dynamically coherent"<sup>13</sup> rotation is evidently ruled out, as already stressed in Ref. 1.

(2) The Gordon's  $J$  diffusion model<sup>14</sup> deserves closer examination because it predicts, if the collisions that it assumes are not too frequent, reasonably long initial inertial behavior for  ${}_1F_u$ , as is observed. Also  $F_J$  in this model can decay not much faster than  ${}_1F_u(t)$ , as again is observed. However, the hard collisions of Gordon's model imply that the initial slope of  $F_J(t)$  is not zero, and that a time sample of  $J^2$  would exhibit a random succession of horizontal plateaus. Both these features

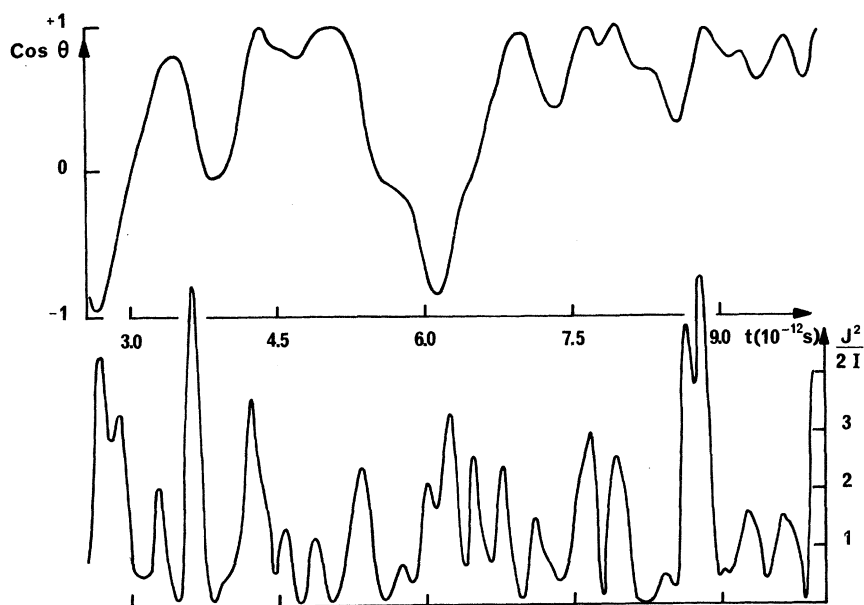


FIG. 11. Sample of the orientational motion of a molecule. Upper curve: cosine of its angle with a fixed axis; lower curves:  $J^2/2I$ , where  $J$  is its angular momentum and  $I$  its moment of inertia. The unit for  $J^2/2I$  is that for the temperature, i.e.,  $\epsilon/k_B$ .

contradict our observations (see our Figs. 7 and 11, respectively). This question is obviously related to the hardness of the repulsive part of the potential. In a recent article<sup>15</sup> Chandler was able to reach a reasonably good agreement with our previous dynamical results on computer-simulated nitrogen, by fitting the nitrogen molecule to a suitably chosen rough hard sphere model. To do this he deduces an equivalent molecular diameter from the observed equilibrium properties, and assumes an arbitrary coefficient for the transfer of angular momentum during collisions. This yields a value for the correlation time of the angular momentum; then, via Gordon's  $J$  diffusion model, the time-correlation functions for the two first spherical harmonics can be computed. As for monatomic liquids, the equivalent molecular diameter which enters into the calculation has to be chosen to be temperature dependent.

In our opinion such a procedure is just an empirical remedy for the fact that the "interval between collision" and the "collision duration" in a dense liquid either cannot be clearly separated or, if, with some arbitrariness, they are separately defined, are of comparable order of magnitude. This point is illustrated by the following approximate calculation: we do not adopt the spherical model, but rather we consider the "collision" of two nitrogen atoms belonging to two different molecules. To take into account the fact that such collisions are brought about by a combination of the translation and the rotational motion of the molecules, we will take the mean kinetic energy per atom to be  $\frac{5}{2}kT$  (since there are five degrees of freedom per molecule). We consider the path of two atoms colliding "head on." We assume that the two atoms are in a "state of collision" if their separation is shorter than  $\sigma$ . The duration of the collision,  $\tau_{CD}$ , is then the time necessary for the path  $\sigma, r_A, \sigma$ , where  $r_A$  is the turning point. On the other hand, from the first peak in the atomic pair-distribution function (Fig. 4 of Ref. 1), the mean atom-atom separation is about  $r_0 = 2^{1/6}\sigma$ . Hence, the mean interval between collisions,  $\tau_{BC}$ , is twice the time necessary for the path  $r_0, \sigma$  because of the statistical symmetry of the environment. Now  $r_A$  is determined by the fact that the time average of the kinetic energy over the total path  $r_0, r_A$  must be  $\frac{5}{4}kT$ . At the triple point one finds  $\tau_{CD} = 0.175 \times 10^{-12}$  sec and  $\tau_{BC} = 0.22 \times 10^{-12}$  sec. These two times are indeed comparable. If one is fond of hard-core models, one may compare their sum ( $0.395 \times 10^{-12}$  sec) with the Enskog time computed for the atomic collisions: again taking  $\sigma$  for the atomic diameter and  $\rho = 2\rho^*/\sigma^3$  for the atomic density, using  $g(\sigma)$  of Ref. 1, and adopting  $\frac{5}{4}kT$  instead of  $\frac{3}{2}kT$  for the mean kinetic energy,

one finds  $\tau_E = 0.29 \times 10^{-12}$  sec.

Because short-duration collisions do not exist, the translational velocity and the angular momentum vary smoothly in time. Remembering that the sum  $\tau_{CD} + \tau_{BC} = 0.395 \times 10^{-12}$  sec is computed for head-on collisions, which reverse the angular momentum, an estimate on this basis of the randomization time for the angular momentum would be some  $0.20 \times 10^{-12}$  sec. The observed value,<sup>1</sup>  $0.17 \times 10^{-12}$  sec is even shorter. This is because intermolecular torques evidently act even during the "collision intervals."

The above very simple remarks could have been made before the development of the MD method. It is satisfying both that they are verified by MD and that Gordon was able to verify the validity of his model only for gases (he had to modify it empirically to reproduce the behavior of liquids).<sup>11</sup>

We have mentioned in Sec. II that hard-core models (e.g., Chandler's fused hard spheres) seem to be a good approximation for computing the equilibrium distribution functions in dense liquid nitrogen. This is not in contradiction with our present affirmation of the nonvalidity of these models for describing the dynamics. This is because of the relative orders of magnitude of the three following lengths: a molecular dimension, say  $\sigma$ ; a mean intermolecular gap, say  $\lambda - \sigma$ , where  $\lambda$  is the mean intermolecular distance; and the range of the repulsive potential for a  $kT$  variation, which is of the order of  $r_0 - r_A$  in the above notations. Because the molecular dimension is some ten times larger than the intermolecular gap, the exact shape of the potential in the gap has not much influence on the local arrangement of the molecules. On the other hand, the short-time dynamics are governed by the space-time trajectory in the gap, whose length is comparable to the range of the potential so that the exact shape of the latter is of paramount importance.

(3) Conventional rotational diffusion by small steps, and also Hill's itinerant oscillator model<sup>16</sup> have to be rejected for computer-simulated nitrogen because of the existence of stages of large-angle continuous rotation. Also our ratio of the correlation times for the first and second spherical harmonics is smaller than 3, the value which arises from the rotational diffusion model.

(4) We turn now to the Ivanov model.<sup>17</sup> Here the rotator is assumed to be trapped most of the time and to perform, at random instants in time, instantaneous angular jumps. If we assimilate the stages of continuous rotation we observe to such jumps, we encounter the fact that, far from being very short, these stages last about as long as the trapping stages. Nevertheless, this model shows some resemblance to the situation we observe: for ex-

ample, for large jumps of random size the ratio of the long time decay rate of  ${}_1F_u$  to that of  ${}_2F_u$  is  $1^{17}$  to  $1.2^{18}$ , a figure which is close to the one we observe.

(5) The model proposed by Lassier and Brot<sup>19</sup> is an improvement over the Ivanov model in that it also includes inertial effects both during trapping (perturbed libration) and during jumps (finite duration of the jumps). Here again the behavior of computer-simulated nitrogen has many features in common with the model. However, the librations during the trapping stages are more erratic, and the observed "jumps" last longer, than in the model.

(6) Anderson and Ullman<sup>20</sup> have put forward a model comprising the following interesting hypothesis: whereas in the jump models the molecular environment is implicitly assumed to vary abruptly to allow jumps to occur, these authors suppose that there exists a continuous distribution of environments (free volume) which evolves smoothly, and that the probability of reorientation of the reference molecule depends on the actual environment. This recalls the situation we have observed, in which there exists a cross correlation between the number of "partners" and the decay rate of the local orientational correlation function. However, for our purpose, this model has the drawback of being essentially "relaxational" in the sense that all inertial effects are completely ignored.

(7) The model proposed recently by Kivelson and

Keyes<sup>21</sup> could probably accommodate the main features of the behavior we observe because it allows extreme as well as intermediate situations for a set of dynamical variables. However, even in its most general version this theory assumes that a quantity analogous to the time derivative of the torque has a white spectrum. We have not computed the ACF for this quantity, but a close examination of the curve for  $J^2$  in Fig. 11 suggests that this hypothesis is probably an oversimplification. This assumption, however, can be empirically useful: for it is equivalent to truncating at the second order a hierarchy of memory functions for the orientational correlation function, and it has been shown that this allows a reasonably good fit of the observed CF.<sup>11</sup>

To conclude this section dealing with the comparison with models, we stress the fact that we have preferred to test directly the basic assumptions of each model rather than to tentatively fit our ACF's with those predicted by the models. Indeed, even if successful such fits do not prove the validity of a model, because many models comprise more than one parameter, if not a free function.

#### ACKNOWLEDGMENT

One of the authors (B. Quentrec) is grateful to Dr. D. Levesque for his help in the numerical work and for stimulating discussions.

\*Laboratoire associé au C.N.R.S.

<sup>1</sup>J. Barojas, D. Levesque, and B. Quentrec, *Phys. Rev. A* **7**, 1092 (1973).

<sup>2</sup>B. Quentrec and C. Brot, *J. Chem. Phys.* **54**, 3655 (1971).

<sup>3</sup>E. F. W. Bader, W. H. Henneker, and P. E. Cade, *J. Chem. Phys.* **46**, 3341 (1967).

<sup>4</sup>H. W. Furumoto and C. H. Shaw, *Phys. Fluids* **7**, 1026 (1964).

<sup>5</sup>J. C. Dore, G. Walford, and D. I. Page, *Mol. Phys.* **29**, 565 (1975).

<sup>6</sup>L. J. Lowden and D. Chandler, *J. Chem. Phys.* **59**, 6587 (1973).

<sup>7</sup>We differ here from some of the conventions of Ref. 1.

<sup>8</sup>It has been recorded on magnetic tape and is kept at the disposal of possible users.

<sup>9</sup>E. M. Horl and L. Martin, *Acta Crystallogr.* **14**, 11 (1961). See also T. H. Jordan, H. W. Smith, W. E. Streib, and W. N. Lipscomb, *J. Chem. Phys.* **41**, 756 (1964), who favor a slightly displaced structure.

<sup>10</sup>V. F. Sears, *Can. J. Phys.* **44**, 1299 (1966).

<sup>11</sup>B. Quentrec and P. Bezot, *Mol. Phys.* **27**, 879 (1974).

<sup>12</sup>Obviously, the trapping stages can occur about any direction on the unit sphere. In Fig. 11, we present a case where it happens to be about  $\theta=0$ , since there, whatever the azimuthal angle, trapping is certain.

<sup>13</sup>W. A. Steele, *J. Chem. Phys.* **38**, 2411 (1963).

<sup>14</sup>R. J. Gordon, *J. Chem. Phys.* **44**, 1830 (1966).

<sup>15</sup>D. Chandler, *J. Chem. Phys.* **60**, 3508 (1974).

<sup>16</sup>N. Hill, *Proc. Phys. Soc. Lond.* **82**, 723 (1963).

<sup>17</sup>E. N. Ivanov, *Zh. Eksp. Teor. Fiz.* **45**, 1509 (1964) [*Sov. Phys.—JETP* **18**, 1041 (1964)].

<sup>18</sup>A. Ben Reuven and E. Zamir, *J. Chem. Phys.* **55**, 475 (1971).

<sup>19</sup>B. Lassier and C. Brot, *Chem. Phys. Lett.* **1**, 581 (1968).

<sup>20</sup>J. E. Anderson and R. Ullman, *J. Chem. Phys.* **47**, 2178 (1967).

<sup>21</sup>D. Kivelson and T. Keyes, *J. Chem. Phys.* **57**, 4599 (1972).